ISSN: 0975-8585

Research Journal of Pharmaceutical, Biological and Chemical Sciences

Preparation, characterization and antimicrobial activities of 2-hydroxy-N'-3-(hydroxyimino)butan-2-ylidene)benzohydrazide and its complexes.

Fathy A. El-Saied[1]*, Mohamad M. E. Shakdofa[2,3], Ahmed N. Al-Hakimi[4,5], Anas Rasras[2], and Ahmed M Elseidy[6].

[1]Department of Chemistry, Faculty of Science, Menoufia University, Shebin El-Kom, Egypt
[2]Department of Chemistry, Faculty of Science and Arts, Khulais, University of Jeddah, Saudi Arabia
[3]Inorganic Chemistry Department, National Research Center, El-Bohouth St., Dokki, Cairo, Egypt
[4]Faculty of Science, Chemistry Department, Qassim University, Qassim, (KSA)
[5]Department of Chemistry, Faculty of Science, Ibb University, Ibb, Yemen
[6]Chemistry Department, Faculty of Science, Al Imam Mohammad Ibn Saud Islamic University (IMSIU) PO Box 5701, Riyadh 11432, Saudi Arabia.

ABSTRACT

A series of twelve metal complexes with 2-hydroxy-N'-3-(hydroxyimino)butan-2-ylidene) benzohydrazide ligand was synthesized and characterized using elemental analyses, IR, NMR, Mass, and UV-Visible spectra. The ligand behaves either as neutral bidentate, monobasic tridentate, monobasic dibasic tetradentate ligand bonded covalenacy via deprotonated oxamato and enolic carbonyl groups as well as coordinated via the azomethine and oxime nitrogen atoms. The synthesized complexes possess a square-pyramidal geometry as in complexes (2-5) and (13) or octahedral as in complex (7-12), while complex (6) has a tetrahedral geometry. The copper(II) complexes (2-5) ESR spectra confirmed that they have a square pyramidal geometry with a dx2-y2 ground state. The synthesized complexes demonstrate a high cytotoxicity against A. niger and the best one was [Zn(H2L)2] (11) with 84% in compare with Nystatin as a positive control, a moderate activity against E. coli and B. subtilis with 77 and 88% respectively for [Ni(H2L)2] (7) as a best result compare with the positive control Amoxicillin.

Keywords: Benzohydrazide, oxime, metal complexes, antimicrobial, hydrazone-oxime

Corresponding author

ISSN: 0975-8585

INTRODUCTION

Schiff bases possess an outstanding importance in inorganic, analytical and medicinal chemistry because of their versatility to form a large variety of stable complexes upon coordination with different transition metal ions [1-3]. Hydrazone ligands represent a class of Schiff base with extra function group characterized by a nitrogen-nitrogen covalent bond that enhances their capability to form more stable metal complexes via reaction with most of transition metal ions [4-5]. Both hydrazide and hydrazone compounds have drawn much concern in order to investigate their structures as well as their enormous biomedical activities as: antioxidant [6], anti-inflammatory, antimalarial [7], anti-trypanosomal, antibacterial [4], analgesic [8], antiplatelet [9], anticonvulsant [10], antitumor [11], and antiviral activities [12]. The presence of active azomethine NHN=CH- protons in these compounds imparts them a major importance as good candidates for the development of new drugs [13-14] . Also, the C=N double bond in hydrazones are of major concern, as they act as a pivotal group for synthesis of organic compounds, metal complexes and organo-catalysis [15]. The carbon atom in the hydrazone moiety possess both nucleophilic and electrophilic character, while both nitrogen atoms are nucleophilic [13, 16]. For these behavior, hydrazones are widely used in organic synthesis as well as designing of new drugs. In parallel to the growing biochemical applications of hydrazide compounds, oxime-containing ligand derivatives represent another esteemed category with high biological implications. Oximes are recognized by presence oxygen atom attached directly to a nitrogen atom containing a pair of free electrons. The recognized biological activity of oxime derivatives is evidently related to the N-OH groups which enhance their ability to chelate metal ions. The −N−OH moiety appears to be flexible to be oxidized, reduced, and conjugated with inorganic and organic moieties. The α-adjacent atom has free electrons imparts oxime character of being involved in nucleophilic displacements reactions via the anionic form N−O. The oximes ligands remarkable ability of forming stable metal complexes with a large number of metal ions, along with the N−OH group affinity to produce a nitroxide radical, defines to a great extent, but not exclusively, the biological as well as the toxicological activity of oximes. For these characteristic, oxime containing compounds demonstrated effective activities in several biomedical applications as: antimicrobial, antimalarial, and anticancer drugs [17-18]. Based on the unique characteristics of oxime, there is a growing interest related to synthesize as well as structural investigating of oximes derivatives in order to develop novel therapeutic medications. Costanzo et al. reported that oximes can inhibit the activity of arginase enzyme. He related that to the ability of the N=OH groups of the oxime to bind the active centers Mn^{2+} in the enzyme structure [19]. In another study, new binary and ternary Cu(I) complexes derived from Benzyl-thiourea ligand have been synthesized and their antibacterial activity on Gram-negative and Gram-positive strains has been evaluated. The prepared metal complexes demonstrated a profound cytotoxicity against both types of bacteria [20]. It was reported that the combination of both oxime and amide groups in the same molecule leads to the formation of more stable chelator by coordination to the metal ions [21]. In the light of these consideration, we reported herein synthesis of new binary metal complexes derived from 2-hydroxy-N'-3-(hydroxyimino)butan-2-ylidene) benzohydrazide.

RESULTS AND DISCUSSION

The obtained metal complexes are colored, air-stable and insoluble in water, ethanol and non-polar solvents. They demonstrated a good solubility character in polar solvents i.e. DMF and DMSO. All prepared metal complexes showed a non-electrolytes nature. The proposed configuration structures [Figure 2-4] goes in consistent with the elemental, thermal and spectral analyses [experimental part and Tables 1-3]. We have not managed to grow diffractable single crystals till now. Complexes **(2)** and **(7-8)** were formed in 1L:1M molar ratio, complexes **(3-4)** and **(12)** formed in molar ratio [2M:2L] while complexes **(5)**, **(6)** and **(9-12)** were adopt ML_2 formulae.

ISSN: 0975-8585

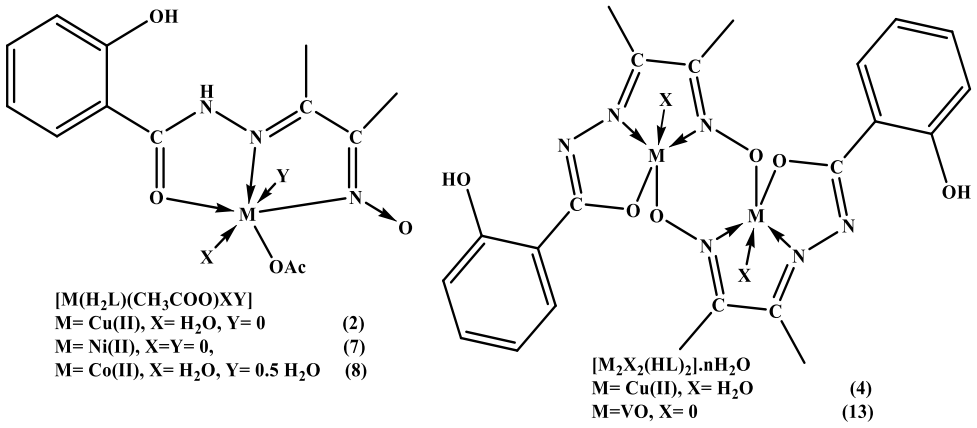

Figure 2: **Suggested structures of Cu(II), Co(II) and Ni(II) complexes 2-4, 6, 8 and 13.**

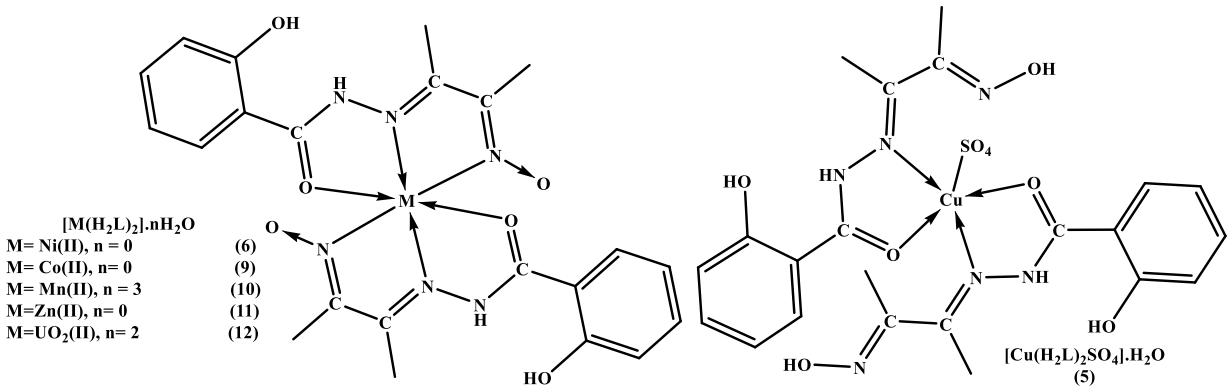

Figure 3: **Suggested structures of Cu(II), Ni(II), Co(II), Mn(II), Zn(II) and UO_2(II) complexes 5, 7 and 9-12.**

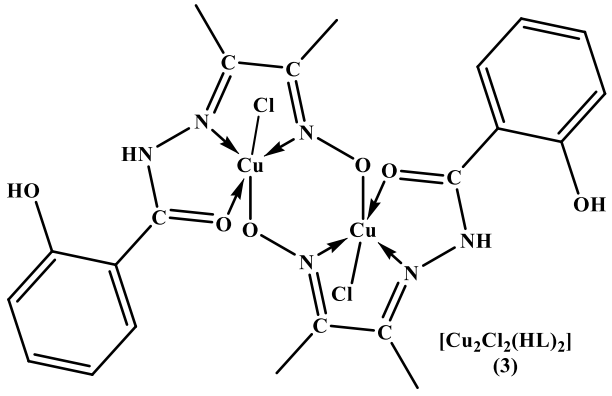

Figure 4: **Suggested structures of Cu(II) complex 3.**

CONDUCTIVITY MEASUREMENTS

The values of molar conductance for 0.001 M of the metal complexes **(2-13)** at 25 ˚C in DMSO are depicted in experimental part. The 3.9-29.7 $\Omega^{-1}cm^2mol^{-1}$values referred to a non-electrolytic nature of these complexes [22]. The high value of some complexes could be related the partial solvolysis of it by solvent molecules.

NMR SPECTRA

The measured ligand **(1)** ^{1}H NMR spectrum (Table 1) at °K utilizing DMSO-d6 as a solvent demonstrated oxime proton at δ = 11.31 ppm while the phenolic OH proton appeared at δ = 11.70 ppm. The amide proton

present at δ = 11.61 ppm, aromatic protons appeared as doublet signal at 7.98 ppm, triplet at 7.42 ppm and multiplet at 7.45-6.96 ppm range and two singlet peaks at 2.14 ppm and 2.05 ppm belong to two methyl groups. The ^{1}H NMR spectrum of complex (**11)** shows phenolic protons shifted to low field at δ = 13.59 ppm, which could be due to intramolecular hydrogen bonding with the carbonyl group, since the carbonyl group is chelated with the metal ion. On the other hand oxime protons are disappeared which clarified that the metal ion is bonded to the oxamato nitrogen atom. The NH proton peak is appeared at δ = 11.64 ppm which support the suggested structure for complex (**11)**. Aromatic protons appeared in the δ = 6.73-7.89 ppm range and two singlet peaks for methyl groups at δ = 2.23 ppm and 2.05 ppm.

Table 1. ^{1}H-NMR data for the ligand H_3L and Zn(II) complex

Groups	Signals (ppm)	
	Ligand (H_3L)	$[Zn(H_2L)_2]$ (11)
δ(OH)	11.70 (s, 1H), 11.31 (s, 1H)	13.59 (s, 2H),
δ (NH)	11.61 (s, 1H)	11.64 (s, 2H)
δ (H-C aromatic)	7.98 (d, 1H), 7.42 (t, 1H), 7.45-6.96 (m, 2H)	7.89-7.72 (m, 2H), 7.31-7.21 (m, 2H), 6.81-6.73 (m, 4H)
δ (CH_3)	2.14 (s, 3H), 2.05 (s, 3H)	2.23 (s, 6H), 2.05 (s, 6H)

INFRARED SPECTRA

The ligand IR spectrum showed a broad peaks at 3560 and 3287 cm^{-1} responsible for OH and NH groups respectively [23-24]. The strong peaks at 1652 cm^{-1} assign to the carbonyl group [23] while 1614 and 1550 cm^{-1} ascribed to ν(C=N) of azomethine and oxime groups [25] respectively. Whilst the two medium peaks appeared at 1078 and 983 cm^{-1} assign to ν(N-O) [26] and ν(N-N) [23-24] respectively . Based on variation complexes IR data in comparison to that of the ligand, it could be presumed that the ligand performed either: a neutral tridentate, monobasic tridentate, dibasic tetradentate or monobasic tetradentate.

The comparison of complexes **(2)** and **(6-12)** spectra revealed that the ligand in these complexes acted as monobasic tridentate fashion bonded covalency via nitrogen atom of deprotonated oxamato group and coordinated through the azomethine and ketonic carbonyl groups. This bonding behavior are supported by the next evidences. i) Complete absence of the ν(OH) of oxime moiety which is confirmed from Zn(II) complex ^{1}H NMR which showed the disappearance of the oxime hydroxyl proton. ii) a negative shift in the intensity and position of azomethine group (17-50 cm^{-1}) iii) a negative shift in the intensity and position of the carbonyl group by (12-52 cm^{-1}) and in the same the appearance of NH bands in the range (3139-3264 cm^{-1} iv) a negative shift in the intensity and position of oxamato group (C=N) by (10-33 cm^{-1}) with a substantial change is also appeared in the N–O stretching which appears in the 1134-1185 cm^{-1}, indicating an increase in the double bond character of the NO bond due to the loss of the hydroxyl hydrogen [25, 27]. v) The new bands which appeared in the 544-592, 517-540 and 459-499 cm^{-1} ranges related to ν(M←O) and ν(M←N) respectively [28-29]. The spectra of the bimetallic complexes **(4)** and **(13)** suggested the ligand chelated to the metal ions in a dibasic tetradentate mode bonding two metal ions through the two nitrogen atoms of imine and oxamato groups, enolic carbonyl oxygen and deprotonated oxamato oxygen. This mode is supported by the following evidences: i) The absence of oxime hydroxyl proton that is confirmed from ^{1}H-NMR of Zn(II) complex which showed the absence of the oxime hydroxyl proton signal ii) a negative shift in the intensity and position of oxamato group (C=N) which appear at 1541 and 1431 cm^{-1} with an essential change is also observed in the N–O stretching that manifests at 1135, 1130 cm^{-1}, referring an increment in the double bond character of the NO bond owing to the hydroxyl hydrogen losing [25, 27]. iii) complete disappearance of the bands of carbonyl group and amino hydrogen (NH) of the hydrazide moiety [23] iv) the appearance of an extra peak at 1522, 1530 cm^{-1} respectively ascribed to the emerging of a new C=N group which is reinforced by the appearance of new bands at 1216, 1245 cm^{-1} corresponding to ν(C-O) of hydrazide moiety [30-31]. v) The occurrence of new peaks in the 592,577; 544, 534; 521, 509 and 467, 470 cm^{-1} related to ν(M-O), ν(M-O), ν(M–N) and ν(M←N)

ISSN: 0975-8585

respectively [28-29]. The spectrum of copper complex **(3)** $[Cu(H_2L)Cl]_2$ show similar patterns except the still presence of the bands characteristic to the carbonyl and NH group of the hydrazide moiety. Although this band was subjected to shifting by a (40 cm^{-1}) inductive that the ligand preformed as monobasic tetradente fashion (Fig. 2). The IR spectral findings of these complexes go consistent with the elemental analyses results suggesting that this group of metal complexes adopts M_2L formulae Fig. 1. The copper complex $[Cu(H_3L)SO_4].H_2O$ **(5)** spectrum revealed that t the still presence of the bands characteristic to the carbonyl and NH group of the hydrazide moiety. Although the band of carbonyl group was subjected to shifting by a (50 cm^{-1}) as well as the azomethine band was subjected to shifting by a (54 cm^{-1}) indicating that the ligand acted as neutral bidentate fashion coordinated to the Cu(II) via the ketonic carbonyl and azomethine groups. Two medium new peaks at 963 and 929 cm^{-1} were detected in spectrum of uranyl complex **(12)** could be related to ν_{sym} and ν_{asym} ν(O=U=O) respectively [32-34] while the new peak observed in spectrum of vanadyl complex **(13)** at 947 may be assigned to V=O [29]. The two bands observed in the spectra of acetate complexes **(2), (7)** and **(8)** at 1555, 1337 (Δ=218), 1545, 1363(Δ=182), 1555, 1353(Δ=202) cm^{-1} were assigned to $\nu_{asym.}(COO^-)$ and $\nu_{sym.}(COO^-)$ of the acetate groups [35-36]. The observed separation value (Δ) (182-218) cm^{-1} between asymmetric and symmetric (COO^-) groups indicates that the acetate acts as a mono-dentate in these complexes [35-36]. IR spectra of the sulfato complex **(4),** revealed new bands at 1160, 1070 assigned to ν_3, 942, 540 assigned to ν_4, and 673, 587 assigned to ν_1 and ν_2 [36-37].

MASS SPECTRUM OF LIGAND (H_3L)

The ligand MS confirms the suggested structure of the ligand (scheme 1). It manifests molecular ion peak m/z at 220 which is compatible with the ligand molecular weight. Furthermore, the ligand splits to various fragments which possessed ion peaks equal to m/z= 203, 175, 162, 124, 114, 106, 98, 86 and 79 which corresponding to $C_{10}H_{11}N_4O$, $C_8H_7N_4O$, $C_8H_8N_3O$, $C_5H_6N_3O$, $C_4H_8N_3O$, C_6H_4NO, $C_3H_4N_3O$, $C_3H_8N_3$, and C_5H_5N respectively (Fig. 5).

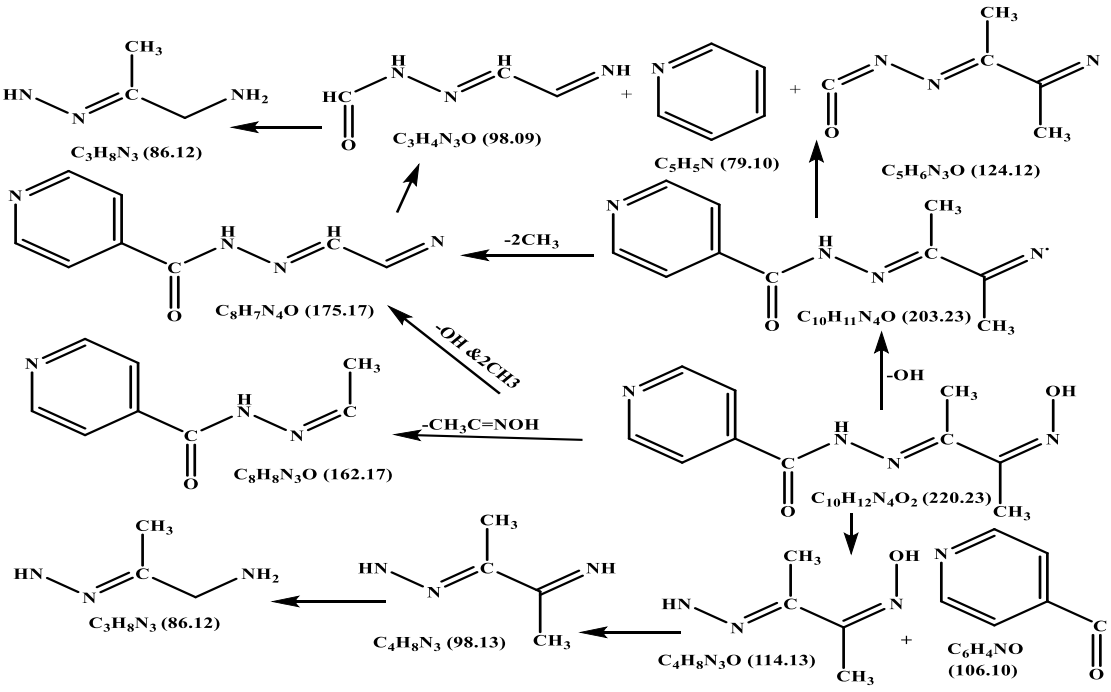

Fig. 5. The fragmentation pattern of the ligand

ELECTRONIC SPECTRA OF LIGAND AND ITS COMPLEXES

The ligand and complexes electronic absorption spectra were done in DMF at 300 °K and reported in Table 2. The ligand electronic absorption spectrum comprises five bands at 264, 280, 288, 308, 375 nm. The two band appeared at 264 nm could be related to the $\pi \rightarrow \pi^*$ transition in the benzoniod moiety [38-39] which do not nearly changed on chelation. Whereas the second peak at 280 nm could be ascribed to hydrogen

bonding [40]. The beaks observed at 288, 308 and 375 nm could be ascribed to n→π* of the azomethine, iminoxime and carbonyl groups respectively [41]. The shifting of these bands in complexes spectrum referring to the involvement of these groups in chelation process. In some complexes, new bands were observed in the 396-430 nm ranges could be related to charge transfer transitions. The Copper(II) complexes **(2-5)** electronic spectra showed three bands in the 1063-1080, 580-619 and 490-545 nm ranges assignable to $(\nu_1)^2B_{1g}\rightarrow{}^2A_{1g}(d_{x2-y2}\rightarrow d_{z2})$, $(\nu_2)^2B_{1g}\rightarrow{}^2B_{2g}(d_{x2-y2}\rightarrow d_{xy})$ and $(\nu_3)^2B_{1g}\rightarrow{}^2E_g(d_{x2-y2}\rightarrow d_{xz},d_{yz})$ transitions supposing that these complexes could be considered to have five-coordinate geometry [Fig. 2][42-44]. The basic arrangements with five coordinated geometry, are square pyramidal (SP) and trigonal bipyramidal (TBP). The two arrangements SP and TBP are recognized by the ground state d_{x2-y2} and d_{z2} respectively. It is impossible distinguish to between these structures based on the electronic spectra only. Hence it is differentiate based on ESR spectra. Ni(II) complexes are capable to form coordination compounds of different stereochemistry viz. square planar, tetrahedral or octahedral. In an octahedral field, the 3F Russel–Saunders term split into three components $^3A_{2g}$, $^3T_{2g}$, and $^3T_{1g}$ in order of increasing energy. ^1D splits into ^1E_g and $^1T_{2g}$, ^3P changes into $^3T_{1g}$, T_{2g} thus spin allowed transitions are possible. The Ni(II) complex **(6)** UV. Vis is compatible with an octahedral stereochemistry around the nickel(II) ion, showing three transitions at 1057, 865, 445 nm. These transitions are assignable to the transitions $^3A_{2g}(F)\rightarrow{}^3T_{2g}(F)$, $^3A_{2g}(F)\rightarrow{}^3T_{1g}(F)$, $^3A_{2g}(F)\rightarrow{}^3T_{1g}(P)$ respectively [43-46]. The ν_2/ν_1 ratio of this complex is 1.22 which is lower than the usual range 1.50–1.75, inductive to distorted octahedral stereochemistry nickel(II) complexes [47]. The nickel(II) complex **(7)** UV. Vis spectrum shows transitions at 1061 and 613 nm corresponding to the $^3A_2(F)\leftarrow{}^3T_1(F)$ and $^3T_1(P)\leftarrow{}^3T_1(F)$ transitions, respectively, which are similar to those substantive for tetrahedral coordinated Ni(II) complexes in the literature [44, 48-50]. Cobalt(II) complexes **(8)** and **(9)** electronic spectra show electronic spectral peaks 1070, 1062; 694, 624 and 499, 510 nm corresponding to the transitions $^4T_{1g}(F)\rightarrow{}^4T^{2g}(F)$, $^4T_{1g}(F)\rightarrow{}^4A_{2g}(F)$ and $^4T_{1g}(F)\rightarrow{}^4T_{1g}(P)$ respectively supposing that these complexes have a six coordinated geometry. The ratio of ν_2/ν_1 are 1.54 and 1.70 which are lower than usual range for an octahedral cobalt(II) (1.95–2.48), inductive to distorted octahedral stereochemistry cobalt(II) complexes. This is compatible with very broad nature of the band which could be ascribed to the envelope of the transitions from $^4E_g(^4T_{1g})$ to the components $^4B_{2g}$ and ^4E_g of $^4T_{2g}$ characteristic of tetragonally-distorted octahedral environment [44, 46, 51-53]. Electronic absorption spectra of Mn(II) octahedral complex are expected to show the following four spin allowed $(\nu_1)^6A_{1g}\rightarrow{}^4T_{1g}(^4G)$ $(\nu_2)^6A1g\rightarrow{}^4E_g(^4G)$, $(\nu_3)^6A_{1g}\rightarrow{}^4E_g(^4D)$ and $(\nu_4)^6A_{1g}\rightarrow{}^4T_{1g}(^4p)$ transitions. The Mn(II) complex **(10)** has exhibited four week absorption bands at 631, 589, 508, and 469 cm^{-1}, which corresponds to ν_1, ν_2, ν_3 and ν_4 transitions respectively, suggesting octahedral geometry for the Mn(II) complex. These transitions are characteristic of a Mn(II) ion in an octahedral environment [44, 54-55]. Zinc(II), uranyl(II) complexes **(11-12)** showed diamagnetic character as expected for d^{10} configuration. They do not show d-d transitions, and the observed bands are only intra-ligand transitions [56-57]. The oxovanadium(IV) complex **(13)** electronic spectrum shows bands at 918, 700 and 490 nm. These bands are attributed to $^2B_2\rightarrow{}^2E$, $^2B_2\rightarrow{}^2B_1$, and $^2B_2\rightarrow{}^2A_2$ transitions which are similar to those of other 5-coordinate oxovanadium(IV) complexes.[58-59] These spectral bands are explicated according to an energy level scheme given by Tsuchimoto et al [60]. The uranium(VI) complex **(12)** electronic spectrum showed two bands at 515 and 426 nm which could be attributed to charge transfer from uranyl oxygen to f-orbital of the uranium(VI) ion. The broadening of this peak referees to the unequal energies of the O→U charge transfer in the two oxo-cations and charger transfer transition from ligand to the uranium(VI) ion [61].

MAGNETIC MOMENTS

The magnetic moment data of polycrystalline metal(II) complexes at 298 °K are shown in Table (2). The data showed that Cu(II), Ni(II), Co(II), Mn(II) and VO(II) are paramagnetic but Zn(II) and UO_2(II) are diamagnetic. The μ_{eff} values for monomeric copper(II) complexes (**2**) and (**5**) are 1.81 and 2.28 BM respectively corresponding to one unpaired electron system (1.73 BM) [62]. The value of complex **(5)** is a little larger than that of a square pyramidal $3d^9$ ion, which should be associated with some orbital contribution [63]. While magnetic-moment value for dimeric copper(II) and vanadyl complexes **(3), (4)** and **(13)** are found to be 1.26, 1.05 and 1.56 BM that is less than the spin only value (1.73 BM) referring to the existence of antiferromagnetic interaction between the two M(II) ions [64]. Nickel(II) complexes (**6**) and (**7**) show μ_{eff} values 3.39 and 3.48 BM, confirmed electronic configuration with two unpaired electrons in an octahedral or tetrahedral nickel(II) complexes [65]. The μ_{eff} values of solid state cobalt(II) complexes (**8**), and (**9**) are 4.54 and 5.89 BM, confirmed electronic configuration with three unpaired electrons in an octahedral cobalt(II) complexes. The subnormal values of these complexes may be explained by weak antiferromagnetic intermolecular interaction between complex molecules [66]. Manganese(II) complexes (**10**) shows values 6.12 BM attributing to a high spin

ISSN: 0975-8585

octahedral Manganese(II) ion [23]. The complexes of Zn(II) and UO_2(II) are diamagnetic as expected and according to these complexes empirical formulae octahedral geometry is proposed for Zn(II) and UO_2(II) complexes.

Table 2.The UV-Vis spectra and magnetic moments for the ligand and its complexes

No.	π–π* , n–π* and CT bands	d–d bands	Transitions	Geometry	μ_{eff}(BM)
1	264, 280, 288, 308, 375	-	--		
2	270, 320, 390, 425	493, 595, 1070	$(\nu_1)^2B_{1g}\rightarrow{}^2A_{1g}(d_{x2-y2}\rightarrow d_{z2})$ $(\nu_2)^2B_{1g}\rightarrow{}^2B_{2g}(d_{x2-y2}\rightarrow d_{xy})$ $(\nu_3)^2B_{1g}\rightarrow{}^2E_g(d_{x2-y2}\rightarrow d_{xz},d_{yz})$	Square pyramidal	1.81
3	268, 380, 425	490, 580, 1080			1.15
4	269, 380, 426,	545, 619, 1076			1.05
5	266, 300, 326, 382, 428	525, 600, 1080			2.28
6	263, 350, 365, 388, 405	445, 865, 1057	$^3A_{2g}(F)\rightarrow{}^3T_{2g}(F)^3A_{2g}(F)\rightarrow{}^3T_{1g}(F)$ $^3A_{2g}(F)\rightarrow{}^3T_{1g}(P)$	octahedral	3.39
7	260, 349, 362, 387, 400	613, 1061	$^3A_2(F)\leftarrow{}^3T_1(F)^3T_1(P)\leftarrow{}^3T_1(F)$	Tetrahedra	3.48
8	264, 277, 321, 372, 420	510, 694, 1070	$^4T_{1g}(F)\rightarrow{}^4T^{2g}(F)$ $^4T_{1g}(F)\rightarrow{}^4A_{2g}(F)$ $^4T_{1g}(F)\rightarrow{}^4T_{1g}(P)$	octahedral	4.54
9	263, 281, 320, 380, 437	499, 624, 1062			5.89
10	263, 304, 354, 430	631, 589, 508, 469	$(\nu_1)^6A_{1g}\rightarrow{}^4T_{1g}(^4G),(\nu_2)^6A1g\rightarrow{}^4E_g(^4G)$ $(\nu_3)^6A_{1g}\rightarrow{}^4E_g(^4D),(\nu_4)^6A_{1g}\rightarrow{}^4T_{1g}(^4p)$	octahedral	6.12
11	263, 380, 382, 423	--	---		Dia
12	261, 276, 289, 305, 364, 426,	---	--		Dia
13	264, 279, 288, 306, 380, 396	503, 821, 919	$^2B_2\rightarrow{}^2E,^2B_2\rightarrow{}^2B_1,$ $^2B_2\rightarrow{}^2A_2$	square pyramidal	1.26

COPPER(II) COMPLEXES ELECTRON SPIN RESONANCE

Copper complexes ESR spectra give more information about the bonding site and geometry of copper complexes. It was measured in polycrystalline state at 298 °k on Varian E-109 spectrophotometer in 3-mm Pyrex tubes at frequency 9.8 GHz and their data listed in Table 3. The copper complexes **(2-5)** are penta-coordinated, there are two basic arrangements with five coordinated geometry, i.e. SP and TBP. The two arrangements SP and TBP are recognized by the ground state d_{x2-y2} and d_{z2}, respectively. Complexes **(2-5)** ESR spectra supply a well base for characterizing between the two ground states d_{x2-y2} and d_{z2}. For a system with $g_{\|}>g_{\perp}$ the geometry is SP but if $g_{\|}<g_{\perp}$ the geometry is TBP [67-69]. However the copper (II) complexes **(2-5)** ESR spectra revealed that the complexes exhibited anisotropic signals with $g_{\|}$, $g_{\perp}$ and g_{iso} values are in the 2.203-2.235, 2.051-2.060 and 2.104-2.119 ranges respectively. These values are typical for a species d^9 configuration with an axial symmetry type of d_{x2-y2} ground state. $g_{\|}$ and $g_{\perp}$values are close to 2.00 and $g_{\|}>g_{\perp}>g_e$(2.0023), stating that all complexes have a square-pyramidal geometry [70]. The $g_{\|}>g_{\perp}$, trend confirmed that the unpaired electron is centralized in d_{x2-y2} orbital and the geometry of these complexes are SP rules out the possibility of a TBP structure that could be predicted to have $g_{\|}<g_{\perp}$ [69, 71]. With respect to Hathaway expression which stated that G= $(g_{\|}-2)/(g_{\perp}-2)$, the exchange coupling interaction between copper(II) ions is negligible if G>4 whereas a significant interaction is present if G<4 [72-73]. The G values of complexes (2) and (5) are 4.27 and 4.24, inductive to the absence of interaction between copper(II) ions [72]. While complexes **(3)** and **(4)** have values 3.54 and 3.89 respectively indicating that there is interaction between two copper(II) ions [72]. Kivelson and Neiman show that the copper(II) complexes $g_{\|}$-values could be utilized as a measure of covalent feature of the bond between the ligand and metal ion. If the $g_{\|}$-value is more than 2.3, the environment is basically ionic but if less than 2.3 referrer to a covalent environment [74]. The $g_{\|}$-values of complexes **(2-5)** are in the 2.203-2.235 range, referring that a significant covalent character is present in complexes **(2-5)** [75]. The g-values could be related to the parallel ($k_{\|}$) and perpendicular ($k_{\perp}$) components of the orbital reduction factor (k) as next equations [76-77].

$$k_{\|}^2 = (g_{\|} - 2.0023)\Delta E_{xy}/8\lambda_o$$
$$k_{\perp}^2 = (g_{\perp} - 2.0023)\Delta E_{xz}/2\lambda_o$$
$$k^2 = (k_{\|}^2 + 2k_{\perp}^2)/3$$

ISSN: 0975-8585

Where λ_o is the spin orbit coupling of the free copper(II) ion (-828 cm^{-1}), ΔE_{xy} and ΔE_{xz} are the electronic transitions $^2B_{1g} \rightarrow {}^2B_{2g}$ and $^2B_{1g} \rightarrow {}^2E_g$ respectively. The calculated values of $k_{||}^2$, $k_{\perp}^2$ and k^2 are in the 0.49-0.606, 0.575-0.711 and 0. 547-0.678 ranges respectively Table 3, showed that, $k_{||}^2 < k^2$ which is a well proof for the presumed $^2B_1$ ground state for the complexes. Furthermore, for ionic environment, k = 1, and for covalent environment k is less than 1. The lower values of k than the unity (0.74-0.822) are indicating of their covalent nature, that is in agreeable with the result gained from the $g_{||}$ values [76-77].

Table 3: - ESR parameters of copper(II) complexes (2-5)

Complex No.	2	3	4	5
$g_{||}$	2.231	2.235	2.203	2.217
$g_{\perp}$	2.054	2.060	2.054	2.051
g_{iso}	2.113	2.119	2.104	2.107
$A_{||}$ (cm^{-1})	177×10^{-4}	146×10^{-4}	154×10^{-4}	140×10^{-4}
$A_{\perp}$ (cm^{-1})	29×10^{-4}	34×10^{-4}	19×10^{-4}	34×10^{-4}
A_{iso} (cm^{-1})	76×10^{-4}	69×10^{-4}	62×10^{-4}	67×10^{-4}
$g_{||}/A_{||}$ (cm^{-1})	126×10^{-4}	153×10^{-4}	143×10^{-4}	159×10^{-4}
G	4.27	3.54	3.89	4.24
ΔE_{xy}(cm^{-1})	16806	17241	16155	16666
ΔE_{xz} (cm^{-1})	19801	20300	18348	19048
$K_{\parallel}^2$	0.581	0.607	0.49	0.541
$K_{\perp}^2$	0.621	0.711	0.575	0.563
K^2	0.608	0.678	0.547	0.555
K	0.7796	0.822	0.74	0.745
□□	0.747	□□□□□	0.638	0.677

The orbital reduction parameters α^2 was calculated from the next equation

$$\alpha^2 = (g_{\parallel} - 2.0023) + \frac{3}{7}(g_{\perp} - 2.0023) - \left(\frac{A_{\parallel}}{P}\right) + 0.04$$

where P is the free ion dipolar term equals 0.036, $A_{\parallel}$ is the parallel coupling constant expressed in cm^{-1}. The α^2 values of the complexes **(2-5)** lie in the 0.638-0.747 range, indicating to a significant degree of covalency in σ-plane [74, 78-79].

THERMAL ANALYSES

Complexes **(2-5), (8), (10)** and **(12)** Thermogravimetric (TG) analysis were recorded in temperature range 25-800 °C to study their thermal behavior. The results tabulated in Table 3. The thermal data revealed that the weight loss of the calculated and the suggested formulae are agreeable. The Thermogravimetric analyses data refer that the **(2-5), (8), (10)** and **(12)** are mostly degraded in two, three or four stages that can be interpreted as nest:

1. Dehydration of complexes **(5), (10)** and **(10)** occur in the 65-105 °C with losing in weight 2.52, 9.66 and 4.90 % corresponding to removal of H_2O **(5),** $3H_2O$ **(10).** $2H_2O$ **(12)**.
2. The second step of complexes **(2), (4)** and **(8)** which occurs in the 110-180 °C with losing in weight 4.02, 5.99 and 7.07 that corresponds to the losing of 1, 2 or 1.5 molecules of coordinated water.

ISSN: 0975-8585

Table 4. The thermal analysis (TG) of complexes (2-5) , (8), (10) and (12)

No.	Temp. range °C	Loss in weight Found (calcd.)	assignment	Composition of the residue
2	125-140	4.02 (4.81)	Loss of one coordinated water molecule (H_2O)	$[Cu(H_2L)(CH_3COO)]$
	160-190	15.71(15.86)	Loss of acetate ion (CH_3COOH)	$[Cu(H_2L)]$
	370-570	56.17(58.11)	Complex decomposition forming CuO	CuO
3	265-305	10.67(10.64)	Loss of two chloride ions (2HCl)	$[Cu\ (H_2L)]_2$
	420-550	62.99 (65.49)	Complex decomposition forming CuO	2CuO
4	110-165	5.99 (5.72)	Loss of coordinated water molecule ($2H_2O$)	$[Cu(HL)]_2$
	400-585	65.04(69.01)	Complex decomposition forming CuO	2CuO
5	70-95	2.52 (2.78)	Dehydration process ($1H_2O$)	$[Cu(H_3L)(SO_4)]$
	215-265	14.68 (14.81)	Loss of one sulfate ion (H_2SO_4)	$[Cu(H_3L)]$
	370-590	69.19 (70.13)	Complex decomposition forming CuO	CuO
8	115-185	7.07 (7.13)	Loss of coordinated water molecule ($1.5H_2O$)	$[Co(H_2L)(CH_3COO)]$
	220-285	15.55(15.67)	Loss of acetate ion (CH_3COOH)	$[Co(H_2L)]$
	370-665	55.21(57.44)	Complex decomposition forming NiO	CoO
10	75-105	9.66 (9.36)	Dehydration process ($3H_2O$)	$[Mn(H_2L)_2]$
	330-500	58.13(60.87)	Complex decomposition forming MnO	MnO
12	65-105	4.90 (4.65)	Dehydration process ($2H_2O$)	$[UO_2(H_2L)_2]$
	350-467	55.75(58.42)	Complex decomposition forming UO_3	UO_3

3. 3.The elimination of coordinated anions acetate, chloride or sulfate from complex (2), (8), (3) and (5) take place in the 160-285 °C which can be confirmed from the percentage weight loss (Table 4).
4. 4.The last stage is the complete degradation of (2-5), (8), (10) and (12) through disintegration of the organic ligand in the 350-590 °C leaving the metal oxide which can be confirmed from the percentage weight loss (Table 4).

ANTIMICROBIAL ACTIVITY:

The test was performed using Well Diffusion Method at 10 mg/mL concentration in DMSO [80-81]. The inhibition zones caused by the different compounds on the microorganisms were tested. The screening results are shown in Table 5. It showed that all the tested complexes were active against the three microorganisms. From the data, it is clear that compounds $Cu(H_2L)(CH_3COO)(H_2O)]$ (**2**), $[Ni(H_2L)_2]$ (**6**), $[[Zn(H_2L)_2]$ (**11**), $[[UO_2(H_3L)_2].2H_2O$ (**12**) and $[VO(HL)0.5H_2O)]$ (**13**) were the highest activity against *A. niger* with 84% for complex **11** and 80% for the others compare with the antifungal Nystatin. Against *E. coli*. Compounds $[Ni(H_2L)(CH_3COO)]$ (**7**), $[Co(H_2L)_2]$ (**9**) and $[[UO_2(H_3L)_2].2H_2O$ (**12**) showed the best results with 77, 71 and 74% respectively compare with the Amoxicillin as antibacterial agent. On the other hand, $[Cu(H_3L)(SO_4(H_2O)]$ (**5**), $[Ni(H_2L)(CH_3COO)]$ (**7**) and $[Mn(H_3L)_2(CH_3COO)_2].3H_2O$ (**10**) were found to have the highest activity against the strains *B. subtilis* with 73, 88 and 78% compared with Amoxicillin as antibacterial agent. The ligand H_3L (**1**) was active against only *E. coli* with 31% compare with the Amoxicillin.

Table 5. Biological activities of the ligand and its metal complexes against bacteria and fungus

No.	A. niger	Activity Index (%)	E. coli-	Activity Index (%)	B. subtilis+	Activity Index (%)
DMSO	0	0%	0	0%	0	0
Nystatin	25	100%	--	--	--	--
Amoxicillin	--	--	35	100%	40	100%
1	0	0%	11	31%	0	0%
2	20	80%	17	49%	23	58%
3	18	72%	22	63%	28	70%
4	16	64%	23	66%	25	63%

5	17	68%	24	69%	29	73%
6	20	80%	19	54%	24	60%
7	19	76%	27	77%	35	88%
8	15	60%	20	57%	29	73%
9	15	60%	25	71%	25	63%
10	19	76%	21	60%	31	78%
11	21	84%	22	63%	23	58%
12	20	80%	26	74%	19	48%
13	0	0%	30	86%	16	40%

2. EXPERIMENTAL

Materials

All chemicals used to in this work were of the analytical grade available and used without further purification. 2,3-Butanedione monooxime (assay ≥ 98%), Methyl 2-hydroxybezoate, hydrazine monohydrate were provided from Sigma-Aldrich company; DMSO (assay 99.7%); absolute ethanol (assay ≥ 99.8%). Metal salts; $Cu(CH_3COO)_2.H_2O$, $CuCl_2.2H_2O$, $Cu(NO_3)_2.2.5H_2O$, $Cu(SO_4).5H_2O$, $Ni(CH_3COO)_2.4H_2O$, $Co(CH_3COO)_2.4H_2O$, $Mn(CH_3COO)_2.4H_2O$, $Zn(CH_3COO)_2.2H_2O$ triethylamine (TEA) were provided from SIGMA-ALDRICH company with purity from 98 to 99.99%. $UO_2(CH_3COO)_2.2H_2O$ and $VOSO_4$ (assay ≥ 99.9 %), were provided from American-Elements. 2-hydroxybenzohydrazide was synthesized according to a published procedures [82]. TLC was utilized to assert the purity of obtained compounds.

Instrumentation and measurement

The C, H and N content in the obtained compounds was analyzed at the Microanalytical Laboratory, Cairo University, Egypt. Metal ion content was determined using Standard analytical methods [83-85]. Jasco FT/IR 300E Fourier transform infrared spectrophotometer covering the range 400-4000 cm^{-1} was used to record FT-IR spectra of the ligand and its metal complexes using KBr discs. Electronic absorption spectra were recorded on a Shimadzu UV-2600 spectrophotometer using 1-cm quartz cells taking DMSO as solvent covering the range 190-1100 nm. The thermal analysis (TG) was recorded on a Shimadzu DT-30 thermal analyzer in the temperature range from (room temperature to 800 ºC) at a heating rate of 10 ºC/min. The magnetic susceptibilities of the solid complexes were measured in a borosilicate tube with a Johnson Matthey Magnetic susceptibility Balance at room temperature using the modified Gouy method using mercuric tetrathiocyanatocobaltate(II) as the magnetic susceptibility standard. Diamagnetic corrections were estimated from Pascal's constant [86]. Values of magnetic moments were derived from the equation: $\mu_{eff=2.84}\sqrt{\chi_M^{corr}}_T$ The molar conductance of 10^{-3} M solution of the complexes in DMSO was measured at 25ºC with a Bibby conductometer type MCl. The resistance measured in ohms and the molar conductivities were calculated according to the equation: $\Lambda_M = \frac{V \times K \times g}{Mw \bullet \Omega}$ where: Λ_M = molar conductivity /$\Omega^{-1}cm^2mol^{-1}$, V = volume of the complex solution/ mL, K = cell constant (0.92/ cm^{-1}), Mw = molecular weight of the complex, g = weight of the complex/g, Ω = resistance/Ω. ^{1}H NMR spectrum was obtained on JEOL ECA-500 MHz FT-NMR spectrometer in d_6-DMSO as solvent. The solid ESR spectra of the complexes were recorded with Varian E-109 spectrophotometer in 3-mm Pyrex tubes at 298 ^oK. Diphenyl picrylhydrazide (DPPH) used as a g-marker for the calibration of the spectra.

Synthesis of ligand 2-hydroxy-N'-3-(hydroxyimino)butan-2-ylidene)benzohydrazide

The 2-hydroxy-N'-3-(hydroxyimino)butan-2-ylidene)benzohydrazide was synthesized by mixing 0.001 mol (0.152 g) of 2-hydroxybenzohydrazide in round bottomed flask contains 30 ml ethanol and to 0.001 mol (0.101 g) of 3-(hydroxyimino)butan-2-one in ethanol was added slowly under stirring. The mixture was refluxed for about 3 h. Followed by cooling to room temperature. After cooling, the white solid precipitate was filtered off and washed with hot ethanol and used for the next step. Yield 90%, m.p. 264 ^oC, color is white.

ISSN: 0975-8585

Elemental microanalyses, Calcd. (%) for ligand (H_3L)= $C_{11}H_{13}N_3O_3$ (FW = 235.1): C, 56.16; H, 5.57; N, 17.86. Found (%) C, 66.11; H, 5.54; N, 17.86. IR data, 3560, 3287, 1652, 1614, 1550, 1078, 983 cm^{-1} assigned to ν(OH/H_2O, C=O, C=N_{azom}, C=N_{oxime}, O←N and N-N). ^1H NMR (DMSO-d6, 270 MHz). δ= 11.70 (s, 1H, OH_{phenol}), 11.31 (s, 1H, OH_{oxime}), 11.61 (s, 1H, NH), 7.98 (d, 1H, CH aromatic), 7.42 (t, 1H, CH aromatic), 7.45-6.96 (m, 2H, CH aromatic) 2.14 (s, 3H, CH_3), 2.05 (s, 3H, CH_3). The mass spectrum of the ligand (H_2L) revealed molecular ion peak at m/z 235.24.

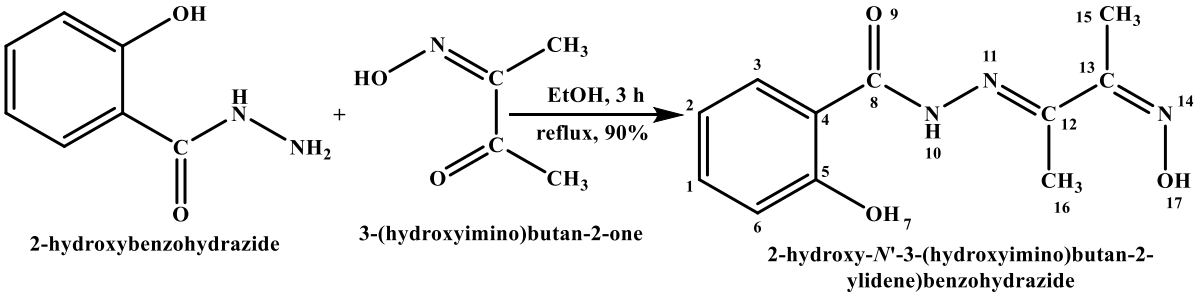

Scheme 1: Synthesis of the 2-hydroxy-N'-3-(hydroxyimino)butan-2-ylidene)benzohydrazide (H_3L)

Synthesis of metal complexes

Metal complexes **(2-4), (6), (8)** and **(13)** were synthesized by reaction of equimolar amount of the following salts: $Cu(CH_3COO)_2.H_2O$, $CuCl_2.2H_2O$, $Cu(NO_3)_2.2.5H_2O$, $Ni(CH_3COO)_2.4H_2O$, $Co(CH_3COO)_2.4H_2O$, $VOSO_4$, respectively with a suitable amount of the ligand in ethanol solution, 5 drops of triethylamine (TEA) was added to the reacting solution after two hours then the refluxing process continued for another one hour. The formed precipitates were filtered off, washed with ethanol, then with diethyl ether and dehydrated under vacuum over anhydrous $CaCl_2$. The same procedures were used to prepare complexes; **(5), (7)** and **(9-12)** using the following metal salts $Cu(SO_4).5H_2O$, $Ni(CH_3COO)_2.4H_2O$, $Co(CH_3COO)_2.4H_2O$, $Mn(CH_3COO)_2.4H_2O$, $Zn(CH_3COO)_2.2H_2O$, $UO_2(CH_3COO)_2.2H_2O$ respectively but in 2 metal: 1 ligand molar ratio.

Complex (2): Yield: 77 %; m.p. > 300 °C; color: Dark green; molar conductivity (Λm): 14.1 ohm^{-1} cm^2 mol^{-1} *Elemental Anal.* Calcd. for [Cu(H_2L)(CH_3COO)(H_2O)] (FW 374.84): C, 41.66; H, 4.57; N, 11.21; Cu, 16.95. Found: C, 54.40; H, 5.41; N, 10.91; Cu, 16.39. IR (KBr, cm^{-1}), 3440 (br), 3230, 1612, 1578, 1530, 1555/1337 (Δ = 218 cm^{-1}), 1163, 556, 533, 489 assigned to ν(OH/H_2O, NH, C=O, C=N_{azom}, C=N_{oxime}, νCH_3COO, O←N, N-N, Cu←O, Cu-N). Cu←N).

Complex (3): Yield: 67 %; m.p. 285 °C; color: Dark green; molar conductivity (Λm): 7.3 ohm^{-1} cm^2 mol^{-1} *Elemental Anal.* Calcd. for $[Cu(H_2L)Cl]_2$ (FW 666.46): C, 39.65; H, 3.63; N, 12.61; Cl, 10.64; Cu, 19.07. Found: C, 39.90; H, 3.74; N, 12.81; Cl, 10.11; Cu, 18.88. IR (KBr, cm^{-1}) 3405, 3191, 1612, 1588, 1540, 1170, 592, 544, 520/467 assigned to ν(OH, NH, C=O, C=N_{azom}, C=N_{oxime}, O←N, N-N, Cu-O, Cu←O, Cu←N).

Complex (4): Yield: 63 %; m.p. >300 °C; color: Dark green; molar conductivity (Λm): 5.9 ohm^{-1} cm^2 mol^{-1} *Elemental Anal.* Calcd. for $[Cu(H_2L)H_2O]_2$. (FW 629.56): C, 41.97; H, 4.61; N, 13.35; Cu, 20.19. Found: C, 41.60; H, 4.25; N, 13.19; Cu, 20.01. IR (KBr, cm^{-1}), 3440, 1589, 1541, 1522/ 1216, 1135, 1023, 592/571, 521/468 assigned to ν(OH/H_2O, NH, C=O, C=N_{azom}, C=N_{oxime}, N=C-O, O←N, N-N, Cu-O, Cu←N).

Complex (5): Yield: 58 %; m.p. >300 °C; color: Dark green; molar conductivity (Λm): 25.9 ohm^{-1} cm^2 mol^{-1} *Elemental Anal.* Calcd. for $[Cu(H_3L)_2(SO_4)].H_2O$. (FW 648.10): C, 40.77; H, 4.35; N, 12.97; Cu, 9.80. Found: C, 40.22; H, 4.53; N, 13.01; Cu, 10.01. IR (KBr, cm^{-1}), 3396, 3282/3218, 1602, 1560, 1545, 1080, 1023, 524, 469 assigned to ν(H_2O/OH, NH, C=O, C=N_{azom}, C=N_{oxime}, O-N, N-N, Cu←O, Cu←N).

Complex (6): Yield: 57 %; m.p. > 300 °C; color: Beige; molar conductivity (Λm): 4.4 ohm^{-1} cm^2 mol^{-1} *Elemental Anal.* Calcd. for $[Ni(H_2L)_2]$ (FW 527.16): C, 50.13; H, 4.59; N, 15.94; Ni, 11.13. Found: C, 50.00; H, 4.45; N, 15.22; Ni, 10.71. IR (KBr, cm^{-1}), 3450, 3213/3171, 1603, 1578, 1540, 1153, 1023, 574/539, 480 assigned to ν(OH, N-H, C=O, C=N_{azom}, C=N_{oxime}, O-N, N-N, Ni-O, Ni-N, Ni←N).

Complex (7): Yield: 66 %; m.p. > 300 °C; color: Light brown; molar conductivity (Λm): 12.6 ohm^{-1} cm^2 mol^{-1} *Elemental Anal.* Calcd. for [Ni(H_2L)(CH_3COO)] (FW 351.97): C, 44.36; H, 4.30; N, 11.97; Cu, 16.68. Found: C,

44.97; H, 4.44; N, 11.91; Ni, 16.11. IR (KBr, cm^{-1}), 3417(br), 3216, 1603, 1563, 1523, 1545/1363 (Δ = 182 cm^{-1}), 1156, 1029, 578, 540, 489 assigned to ν(OH, N-H, C=O, C=N_{azom}, C=N_{oxime}, CH_3COO, O←N, N-N, Ni←O, Ni-N, Ni←N).

Complex (8): Yield: 63 %; m.p. > 300 °C; color: Brown; molar conductivity (⍰m): 10.6 ohm^{-1} cm^2 mol^{-1} *Elemental Anal.* Calcd. for [Co(H_2L)(CH_3COO).1.5H_2O] (FW 379.23): C, 41.17; H, 4.78; N, 11.08; Co, 15.54. Found: C, 41.45; H, 4.67; N, 10.88; Co, 15.11. IR (KBr, cm^{-1}), 3435/3359(br), 3234(br), 1605, 1585, 1533, 1555/1353 (Δ = 200 cm^{-1}), 1152, 1025, 575, 531, 482 assigned to ν(OH/H_2O, NH, C=O, C=N_{azom}, C=N_{oxime},CH_3COO, O←N, N-N, Co←O, Co-N, Co←N).

Complex (9): Yield: 60 %; m.p. 280 °C; color: Brown; molar conductivity (⍰m): 9.1 ohm^{-1} cm^2 mol^{-1} *Elemental Anal.* Calcd. for [Co(H_2L)$_2$] (FW 527.40): C, 50.10; H, 4.59; N, 15.94; Co, 11.17. Found: C, 49.63; H, 4.72; N, 15.51; Co, 10.67. IR (KBr, cm^{-1}), 3440, 3216, 1600, 1570, 1522, 1143, 1021, 561, 525, 499 assigned to ν(OH, N-H, C=O, C=N_{azom}, C=N_{oxime}, O←N, N-N, Co←O, Co-N, Co←N).

Complex (10): Yield: 55 %; m.p. 289 °C; color: Light Brown; molar conductivity (⍰m): 7.2 ohm^{-1} cm^2 mol^{-1} *Elemental Anal.* Calcd. for [Mn(H_2L)$_2$].3H_2O (FW 577.45): C, 45.76; H, 5.24; N, 14.55; Mn, 9.51. Found: C, 45.16; H, 5.55; N, 11.87; Co, 7.56. IR (KBr, cm^{-1}), 3435(br)/3359, 3264/3187, 1605, 1585, 1536, 1153, 1024, 572, 515, 479 assigned to ν(OH/H_2O, NH, C=O, C=N_{azom}, C=N_{oxime}, O←N, N-N, Mn←O, Mn-N, Mn←N).

Complex (11): Yield: 78 %; m.p. >300 °C; color: Yellow; molar conductivity (⍰m): 6.2 ohm^{-1} cm^2 mol^{-1} *Elemental Anal.* Calcd. for [Zn(H_2L)$_2$] (FW 533.85): C, 49.50; H, 4.53; N, 15.74; Zn, 12.25. Found: C, 49.63; H, 4.72; N, 15.33; Zn, 11.78. IR (KBr, cm^{-1}), 3423(br), 3234/3169, 1604, 1565, 1531, 1156, 1022, 579, 535, 494 assigned to ν(OH, N-H, C=O, C=N_{azom}, C=N_{oxime}, O-N, N-N, Zn←O, Zn-N, Zn←N).); ^{1}H NMR (270 MHz, DMSO-d_6): δ= 13.59 (s, 2H, OH_{phenol}), 11.64 (s, 2H, NH), 7.89-7.72 (m, 2H, CH, aromatic), 7.31-7.21 (m, 2H, CH, aromatic), 6.81-6.73 (m, 4H, CH, aromatic), 2.23 (s, 6H, CH_3), 2.05 (s, 6H, CH_3) ppm.

Complex (12): Yield: 81 %; m.p. >300 °C; color: Dark Yellow; molar conductivity (⍰m): 8.5 ohm^{-1} cm^2 mol^{-1} *Elemental Anal.* Calcd. for [UO_2(H_2L)$_2$].2H_2O (FW 774.53): C, 34.12; H, 3.64; N, 10.85; U, 30.73. Found: C, 34.25; H, 4.54; N, 10.31; U, 29.11. IR (KBr, cm^{-1}), 3423, 3255/3139, 1640, 1597, 1517, 1045, 1017, 544/517, 459 assigned to ν(OH/H_2O, NH, C=O, C=N_{azom}, C=N_{oxime}, O-N, N-N, U←O, U-N, U←N).

Complex (13): Yield: 77 %; m.p. 257 °C; color: Gray; molar conductivity (⍰m): 3.9 ohm^{-1} cm^2 mol^{-1} *Elemental Anal.* Calcd. for [VO(HL)]$_2$ (FW 600.34): C, 44.02; H, 3.69; N, 14.00; V, 16.97. Found: C, 43.60; H, 3.96; N, 13.59; V, 16.89. IR (KBr, cm^{-1}), 1598, 1561, 1530, 1130, 1011, 550/509, 470 assigned to ν(OH/H_2O, C=N_{azom}, C=N_{oxime}, N=C-O, O←N, N-N, V-O, V←N).

Biological activities

Evaluation of the antibacterial and antifungal activates of the synthetic ligand and its metal complexes were carried out in the Lab. of microbiology, Botany Department, Faculty of Science, El-Menoufia University against *Escherichia coli* (*E. coli*), *Bacillus subtitles* (*B. subtitles*) and *Aspergillus niger* (*A. niger*) using Well Diffusion Method at 10 mg/mL concentration in DMSO [80-81]. DMSO was used as a negative control, whereas Nystatin and Amoxicillin were used as standard antifungal and antibacterial drugs respectively. The bacteria and fungi were subcultured in a nutrient agar and Czapek Dox´s mediums respectively. The growth inhibition zones around the holes were recorded in millimeters. All determination was made in duplicate for each compound. An average of the two independent readings for each compound was record. The activity index for the complexes was calculated by following formula (3) [87].

$$Activity\ index = \frac{Diameter\ of\ inhibation\ zone\ by\ test\ compound}{Diameter\ of\ inhibation\ zone\ by\ standard} \times 100$$

REFERENCES

[1] Correia I, Adão P, Roy S, Wahba M, Matos C, Maurya MR, Marques F, Pavan FR, Leite CQF, Avecilla F, Costa Pessoa J. Journal of Inorganic Biochemistry. 2014; 141: 83-93.

[2] Ahmadzadeh R, Azarkish M, Sedaghat T. Journal of the Mexican Chemical Society. 2014; 58: 173-179.
[3] Subha L, Balakrishnan C, Natarajan S, Theetharappan M, Subramanian B, Neelakantan MA. Spectrochimica Acta - Part A: Molecular and Biomolecular Spectroscopy. 2016; 153: 249-256.
[4] Anacona JR, Rangel V, Loroño M, Camus J. Spectrochimica Acta Part A: Molecular and Biomolecular Spectroscopy. 2015; 149: 23-29.
[5] Turan N, Gündüz B, Körkoca H, Adigüzel R, Çolak N, Buldurun K. Journal of the Mexican Chemical Society. 2014; 58: 65-75.
[6] Caro AA, Commissariat A, Dunn C, Kim H, García SL, Smith A, Strang H, Stuppy J, Desrochers LP, Goodwin TE. Biochimica et Biophysica Acta (BBA) - General Subjects. 2015; 1850: 2256-2264.
[7] Tsafack A, Loyevsky M, Ponka P, Ioav Cabantchik Z. Journal of Laboratory and Clinical Medicine. 1996; 127: 574-582.
[8] Gökçe M, Utku S, Küpeli E. European Journal of Medicinal Chemistry. 2009; 44: 3760-3764.
[9] Jordão AK, Ferreira VF, Lima ES, de Souza MCBV, Carlos ECL, Castro HC, Geraldo RB, Rodrigues CR, Almeida MCB, Cunha AC. Bioorganic & Medicinal Chemistry. 2009; 17: 3713-3719.
[10] Ragavendran JV, Sriram D, Patel SK, Reddy IV, Bharathwajan N, Stables J, Yogeeswari P. European Journal of Medicinal Chemistry. 2007; 42: 146-151.
[11] Cui J, Liu L, Zhao D, Gan C, Huang X, Xiao Q, Qi B, Yang L, Huang Y. Steroids. 2015; 95: 32-38.
[12] El-Sabbagh OI, Rady HM. European Journal of Medicinal Chemistry. 2009; 44: 3680-3686.
[13] Verma G, Marella A, Shaquiquzzaman M, Akhtar M, Ali MR, Alam MM. Journal of Pharmacy and Bioallied Sciences. 2014; 6: 69-80.
[14] Nogueira VDS, Ramalho Freitas MC, Cruz WS, Ribeiro TS, Resende JALC, Rey NA. Journal of Molecular Structure. 2016; 1106: 121-129.
[15] Özdemir ÜÖ, Akkaya N, Özbek N. Inorganica Chimica Acta. 2013; 400: 13-19.
[16] Ali MR, Marella A, Alam MT, Naz R, Akhter M, Shaquiquzzaman M, Saha R, Tanwar O, Alam MM, Hooda J. Indonesian Journal of Pharmacy. 2012; 193-202.
[17] Hwang T-L, Wang W-H, Wang T-Y, Yu H-P, Hsieh P-W. Bioorganic & Medicinal Chemistry. 2015; 23: 1123-1134.
[18] Sundararajan G, Rajaraman D, Srinivasan T, Velmurugan D, Krishnasamy K. Spectrochimica Acta - Part A: Molecular and Biomolecular Spectroscopy. 2015; 139: 108-118.
[19] Di Costanzo L, Moulin M, Haertlein M, Meilleur F, Christianson DW. Archives of biochemistry and biophysics. 2007; 465: 82-89.
[20] Chetana PR, Srinatha BS, Somashekar MN, Policegoudra RS. Journal of Molecular Structure. 2016; 1106: 352-365.
[21] Sliva TY, Kowalik-Jankowska T, Amirkhanov VM, Glowiak T, Onindo CO, Fritskii IO, Kozlowski H. Journal of Inorganic Biochemistry. 1997; 65: 287-294.
[22] Geary WJ. Coordination Chemistry Reviews. 1971; 7: 81-122.
[23] Fouda MFR, Abd-Elzaher MM, Shakdofa MME, El Saied FA, Ayad MI, El Tabl AS. Transition Metal Chemistry. 2008; 33: 219-228.
[24] Butler IS, Elsayed SA, El-Hendawy AM, Mostafa SI, Jean-Claude BJ, Todorova M. Bioinorganic Chemistry and Applications. 2010; 2010.
[25] Naskar S, Naskar S, Mondal S, Majhi PK, Drew MGB, Chattopadhyay SK. Inorganica Chimica Acta. 2011; 371: 100-106.
[26] Uğur A, Mercimek B, Özler MA, Şahin N. Transition Metal Chemistry. 2000; 25: 421-425.
[27] Mustafa B, Satyanarayana S. Journal of the Korean Chemical Society. 2010; 54: 687-695.
[28] El-Tabl AS, Plass W, Buchholz A, Shakdofa MME. Journal of Chemical Research. 2009; 582-587.
[29] Anitha C, Sheela CD, Tharmaraj P, Sumathi S. Spectrochimica Acta - Part A: Molecular and Biomolecular Spectroscopy. 2012; 96: 493-500.
[30] Chitrapriya N, Sathiya Kamatchi T, Zeller M, Lee H, Natarajan K. Spectrochimica Acta - Part A: Molecular and Biomolecular Spectroscopy. 2011; 81: 128-134.
[31] Galić N, Rubčić M, Magdić K, Cindrić M, Tomišić V. Inorganica Chimica Acta. 2011; 366: 98-104.
[32] Davidson G, Spectroscopic properties of inorganic and organometallic compounds, Royal society of chemistry, Newcastle upon tyne UK, 1993.
[33] Singh B, Mahajan S, Sheikh HN, Kalsotra BL. Journal of Saudi Chemical Society. 2014; 18: 494-501.
[34] Haworth DT, Kiel GY, Proniewicz LM, Das M. Inorganica Chimica Acta. 1987; 130: 113-115.
[35] Murukan B, Mohanan K. Transition Metal Chemistry. 2006; 31: 441-446.

[36] Nakamoto K, Infrared and Raman Spectra of Inorganic and Coordination Compounds Part B: Applications in Coordination, Organometallic, and Bioinorganic Chemistry, Sixth Edition ed., John Wiley & Sons, INC., USA, 2009.
[37] Papatriantafyllopoulou C, Raptopoulou CP, Terzis A, Janssens JF, Perlepes SP, Manessi-Zoupa E. Zeitschrift fur Naturforschung - Section B Journal of Chemical Sciences. 2007; 62: 1123-1132.
[38] Gup R, Kirkan B. Spectrochimica Acta - Part A: Molecular and Biomolecular Spectroscopy. 2005; 62: 1188-1195.
[39] Maurya MR, Agarwal S, Bader C, Rehder D. European Journal of Inorganic Chemistry. 2005; 147-157.
[40] Fouda MFR, Abd-Elzaher MM, Shakdofa MM, El-Saied FA, Ayad MI, El Tabl AS. Journal of Coordination Chemistry. 2008; 61: 1983-1996.
[41] El Bahnasawy RM, El-Tabl AS, Shakdofa MME, El-Wahed NMA. Chinese Journal of Inorganic Chemistry. 2014; 30: 1435-1450.
[42] Bhattacharyya S, Kumar SB, Dutta SK, Tiekink ERT, Chaudhury M. Inorganic Chemistry. 1996; 35: 1967-1973.
[43] Sathyanarayana DN, Electronic absorption spectroscopy and related techniques, Orient BlackSwan Universities press, India, 2001.
[44] Lever ABP, Inorganic electronic spectroscopy, Elsevier science Pub. Co.,, Amsterdam 1984.
[45] Ibrahim MM, Mersal GAM, Al-Juaid S, El-Shazly SA. Journal of Molecular Structure. 2014; 1056-1057: 166-175.
[46] Xiao-Hui S, Xiao-Zeng Y, Cun L, Ren-Gen X, Kai-Be Y. Transition Metal Chemistry. 1995; 20: 191-195.
[47] El-Tabl AS, Aly FA, Shakdofa MME, Shakdofa AME. Journal of Coordination Chemistry. 2010; 63: 700-712.
[48] Fernández-Souto P, Romero J, García-Vázquez JA, Sousa A, Pérez-Lourido P, Valencia L. Inorganic Chemistry Communications. 2012; 26: 28-30.
[49] Sutton D, Electronic spectra of transition metal complexes, McGraw-Hill, London, New York, 1968.
[50] Satyanarayana S, Nagasundara KR. Synthesis and Reactivity in Inorganic and Metal-Organic Chemistry. 2004; 34: 883-895.
[51] Chandra S, Kumar A. Spectrochimica Acta - Part A: Molecular and Biomolecular Spectroscopy. 2007; 68: 1410-1415.
[52] Chandra S, Sharma S. Transition Metal Chemistry. 2007; 32: 150-154.
[53] El-Tabla AS, El-Bahnasawy RM, Shakdofa MME, Ibrahim Hamdy AEDA. Journal of Chemical Research. 2010; 88-91.
[54] El-Tabl AS, Shakdofa MME, Shakdofa AME. Journal of the Serbian Chemical Society. 2013; 78: 39-55.
[55] Sharma R, Agarwal SK, Rawat S, Nagar M. Transition Metal Chemistry. 2006; 31: 201-206.
[56] Sönmez M. Turkish Journal of Chemistry. 2001; 25: 181-185.
[57] Guha A, Adhikary J, Kumar Mondal T, Das D. Indian Journal of Chemistry - Section A Inorganic, Physical, Theoretical and Analytical Chemistry. 2011; 50: 1463-1468.
[58] Yadava AK, Yadav HS, Yadav US, Rao DP. Turkish Journal of Chemistry. 2012; 36: 624-630.
[59] Sarkar A, Pal S. Inorganica Chimica Acta. 2008; 361: 2296-2304.
[60] Tsuchimoto M, Hoshina G, Yoshioka N, Inoue H, Nakajima K, Kamishima M, Kojima M, Ohba S. Journal of Solid State Chemistry. 2000; 153: 9-15.
[61] El-Saied FA, Shakdofa MME, Al-Hakimi AN. Journal of the Korean Chemical Society. 2011; 55: 444-453.
[62] Lai JW, Chan CW, Ng CH, Ooi IH, Tan KW, Maah MJ, Ng SW. Journal of Molecular Structure. 2016; 1106: 234-241.
[63] Lu Z-L, Duan C-Y, Tian Y-P, You X-Z, Fun H-K, Yip B-C. Polyhedron. 1996; 15: 1769-1774.
[64] Kumar R, Mahiya K, Mathur P. Dalton Transactions. 2013; 42: 8553-8557.
[65] Chandra S, Bargujar S, Nirwal R, Yadav N. Spectrochimica Acta Part A: Molecular and Biomolecular Spectroscopy. 2013; 106: 91-98.
[66] Al-Ne'aimi MM, Al-Khuder MM. Spectrochimica Acta Part A: Molecular and Biomolecular Spectroscopy. 2013; 105: 365-373.
[67] Chandra S, Kumar A. Spectrochimica Acta Part A: Molecular and Biomolecular Spectroscopy. 2007; 68: 1410-1415.
[68] Kumar Y, Sharma M, Singh RP, Chandra S. Synthesis and Reactivity in Inorganic and Metal-Organic Chemistry. 1986; 16: 1089-1101.
[69] Hathaway B, Billing D. Coordination Chemistry Reviews. 1970; 5: 143-207.
[70] Hathaway BJ. Journal of the Chemical Society, Dalton Transactions. 1972; 1196-1199.

[71] Bindu P, Prathapachandra Kurup MR. Transition Metal Chemistry. 1997; 22: 578-582.
[72] Shebl M. Journal of Molecular Structure. 2017; 1128: 79-93.
[73] Tomlinson AAG, Hathaway BJ. Journal of the Chemical Society A: Inorganic, Physical, Theoretical. 1968; 1905-1909.
[74] Kivelson D, Neiman R. The Journal of Chemical Physics. 1961; 35: 149-155.
[75] Abdou S, Shakdofa MM, Whaba MA. Spectrochimica Acta Part A: Molecular and Biomolecular Spectroscopy. 2015; 136: 1941-1949.
[76] Ray RK, Kauffman GB. Inorganica Chimica Acta. 1990; 174: 257-262.
[77] Ray RK, Kauffmann GB. Inorganica Chimica Acta. 1990; 174: 237-244.
[78] Sreeja P, Kurup MP, Kishore A, Jasmin C. Polyhedron. 2004; 23: 575-581.
[79] Swamy B, Swamy JR. Transition Metal Chemistry. 1991; 16: 35-38.
[80] Chohan ZH, Supuran CT. Applied Organometallic Chemistry. 2005; 19: 1207-1214.
[81] Akbar Ali M, Mirza AH, Yee CY, Rahgeni H, Bernhardt PV. Polyhedron. 2011; 30: 542-548.
[82] Shelke VA, Jadhav SM, Shankarwar SG, Munde AS, Chondhekar TK. Bulletin of the Chemical Society of Ethiopia. 2011; 25: 381-391.
[83] Svehla G, Vogel's textbook of macro and semi micro Quantitative inorganic analysis 5th ed., Longman New York, 1979.
[84] Vogel AI, Vogle's Text Book of Quantitative chemical Analysis. 5th ed.; JOHN WIELY & SONS New York, 1989; p. 906.
[85] Holzbecher Z, Divis L, Kral M, Sucha L, Vracil F, Handbook of Organic Reagents in Inorganic Analysis, Ellis Horwood Press, JOHN WILEY & SONS INC, New York, 1976.
[86] Figgis B, Lewis J, Wilkins R. Interscience, New York. 1960; 403.
[87] Zaky R, Ibrahim K, Gabr I. Spectrochimica Acta Part A: Molecular and Biomolecular Spectroscopy. 2011; 81: 28-34.